Korean J. Chem. Eng., **30**(6), 1248-1256 (2013)
DOI: 10.1007/s11814-013-0049-0

Kinetic and equilibrium studies on the biosorption of textile dyes onto *Plantago ovata* seeds

Manickam Periyaraman Premkumar*, Vaidyanathan Vinoth Kumar*, Ponnusamy Senthil Kumar, Palanichamy Baskaralingam*, Vasanthakumar Sathyaselvabala*, Thangaraj Vidhyadevi*, and Subramanian Sivanesan*,†**

*Department of Applied Science & Technology, Environmental Management Laboratory, AC College of Technology, Anna University, Chennai 600 025, India
**Department of Chemical Engineering, SSN College of Engineering, Chennai 603 110, India
(*Received 11 December 2012 • accepted 2 April 2013*)

Abstract−The powdered seeds of *Plantago ovata* (PSPO) were utilized for the removal of Malachite Green (MG) and Rose Bengal (RB) dyes from aqueous media by batch adsorption. The Fourier transform infra red spectroscopy (FTIR) results showed that both the dyes were adsorbed between the cellulose matrices, and this has been verified from the intensifying and narrowing aromatic C-H bending vibration. The morphology of the dye laden adsorbent was studied by scanning electron microscopy (SEM), which showed that the dyes were adsorbed between the cellulose matrices of the adsorbent. The PSPO was found to be very effective for the removal of MG and RB at pH 7, and equilibrium was attained within 200 min. The kinetic study indicated that the rate limiting step for MG and RB adsorption may be chemisorption and intraparticle diffusion. Adsorption equilibrium data were fitted to Langmuir, Freundlich, Redlich-Peterson and Temkin adsorption isotherms. It is inferred from the equilibrium studies that the adsorption of MG follows the Freundlich isotherm and the adsorption of RB follows the Langmuir isotherm. The maximum monolayer adsorption capacity of the PSPO was found to be 86.23 mg/g for MG and 81.23 mg/g for RB, respectively.

Key words: Adsorption, Equilibrium, Kinetics, Malachite Green, *Plantago ovate,* Rose Bengal

INTRODUCTION

Effluents from textile industries contain large quantities of chemical residues, especially dyes which originate from the preliminary textile processing steps [1]. In India, the clothing and textile industries are the key industries that are found concentrated in the Tirupur, Karur and Erode districts of Tamilnadu. The downstream banks of the Noyyal River near the Orathupallam dam receive the untreated effluents discharged from the textile processing units in Erode. The Tirupur zones are pounded by the salt laden dye-house effluents, which are severely contaminating the river water as well as the ground water. Textile wastewater also contains dissolved solids, oil and halogenated organics from other processes like bleaching [2]. Wastewater treatment is a great challenge for the textile industries. Even a low concentration of dye in water is highly toxic to the aquatic ecosystem. This, in turn, will affect all the other ecosystems, and there will be a breakdown in the biodiversity. Hence, the removal of synthetic dyes from the effluents becomes environmentally significant.

The wastewater treatment process is used to enable textile industries to reuse wastewater in textile washing through simple, efficient and cost effective methodologies. Several studies were conducted worldwide in treating textile wastewater, resulting in a number of treatment techniques. In recent years, many methods including coagulation and flocculation [3], reverse osmosis [4], chemical oxidation [5], biological treatment [6], photodegradation [7], and adsorption [8] have been employed for the treatment of wastewater containing dyes. Among the various treatment technologies, the adsorption technique is quite popular due to its simplicity and high efficiency, as well as the availability of a wide range of adsorbents.

Adsorbent grade carbon is cost prohibitive, and both the regeneration and disposal of the used carbon are very difficult. Therefore, there is a growing need to find locally available, low cost and effective materials for the removal of dyes. Natural adsorbents of cellulose origin, the most abundant renewable resource on earth, can overcome the disadvantages of activated carbon.

The plant *Plantago ovata* has a wide number of applications in medicine and food processing [9]. However, the seeds are found to possess a hydrogel property, which has not been studied. This research is a novel approach to study the potential of the seeds of *Plantago ovata* to remove dyes from aqueous media. Two dyes, a cationic dye, Malachite Green (MG), and an anionic dye, Rose Bengal (RB), were chosen as the model dyes for the present adsorption study, as they are widely utilized in the textile industry. The effect of various adsorption parameters, such as solution pH, initial dye concentration, contact time and adsorbent dosage, on dye removal by the PSPO, was investigated. The kinetic data were used to test the different kinetic models such as pseudo-first order, pseudo-second order kinetic equations and intraparticle diffusion to know the adsorption mechanism and also the rate limiting step. Adsorption equilibrium data were used to fit the different adsorption isotherm models such as Langmuir, Freundlich, Redlich-Peterson and Temkin isotherm models to predict the adsorption mechanism.

†To whom correspondence should be addressed.
E-mail: sivanesh1963@gmail.com

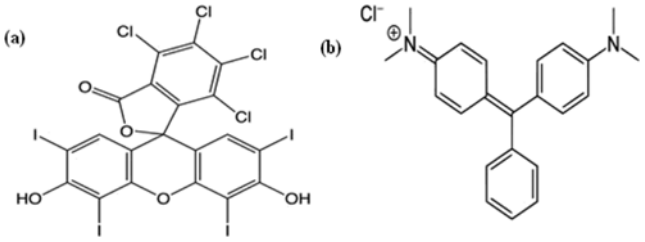

Fig. 1. Chemical structure of (a) rose bengal (RB) and (b) malachite green (MG) dye.

EXPERIMENTAL

1. Materials and Methods

The seeds of the plant *Plantago ovata* were collected from Gujarat, India. Husks and impurities were removed from the seeds by sieving, and the powdered seeds (0.354 mm) were used as the adsorbent. Malachite Green (MG) and Rose Bengal (RB) dyes were procured from Merck (India). Stock solutions of the respective dyes (500 mg/L) were prepared by dissolving the required amount of dye in deionised water. The stock solution was diluted with deionized water to obtain the desired concentrations. The chemical structure of the MG and RB dyes is shown in Fig. 1(a) and Fig. 1(b), respectively.

2. Adsorbent Characterization

The Fourier transform infrared spectrometer (FT-IR) analysis was used to identify the different functional groups present in the adsorbent. The analysis was carried out using the KBr, with the spectral range varying from 4,000 cm^{-1} to 450 cm^{-1}. The surface morphology of the adsorbent was analyzed using a Leo Gemini 1530 scanning electron microscope (SEM) at an accelerating voltage of 15 kV, and at the working distance of 50 μm.

3. Batch Adsorption Experiments

Batch adsorption experiments were carried out by varying the solution pH, the PSPO dose, contact time and initial dye concentration on dye removal. In each experimental study, an accurately weighed quantity of PSPO was added to the respective quantity of dye solution taken in a 250 mL conical flask, and the reaction mixture was agitated at 180 rpm in a horizontal bench shaker (Orbitech). The pH of the solution was maintained at a desired value by adding 0.1 M NaOH or 0.1 M HCl solution. The pH of the solution was measured with a pH meter (Hanna). Once the system approached equilibrium, the samples were centrifuged by using the centrifuge (REMI) to separate the adsorbent, before the residual concentration of dyes in aqueous media was analyzed. The concentration of the dye in the dye solution before and after the adsorption was analyzed, using the UV-Visible spectrophotometer (UV-1800, Shimadzu, Japan). The percentage removal of dyes was calculated by using the following mass balance relationship:

$$\%\text{Dye removal} = \frac{(C_i - C_e)}{C_i} \times 100 \quad (1)$$

where C_i and C_e are the initial and equilibrium concentrations (mg/L) of the dye solution, respectively.

The effect of the solution pH on the adsorption of PSPO was investigated using 50 mL of 100 mg/L dye solution in the pH range between 3 and 10 at 30 °C. The solutions at different pH were agitated in the horizontal bench shaker with 100 mg of PSPO at 180 rpm for 200 min, and then centrifuged to separate the adsorbent. The supernatant was analyzed by using the UV-visible spectrophotometer. In analyzing the effect of the adsorbent dosage on dye removal, we conducted batch adsorption experiments with different adsorbent doses. The PSPO dose was varied from 20 to 140 mg for 100 mL of 100 mg/L dye solution at pH 7, for a contact time of 200 min, at the room temperature of 30 °C. The reaction mixtures were centrifuged, and the supernatants were analyzed as mentioned above. Batch adsorption experiments were carried out at different contact times to analyze the effect of the contact time on the adsorption of MG and RB dyes on the PSPO, and also for kinetic studies. The experimental data were used to test the different kinetic models to know the adsorption mechanism and the rate limiting step. The time varied between 5 and 200 min for an initial concentration of 500 mg/L of dye solution at pH 7, the PSPO dose concentration being 1 g/L, in a 2 L beaker at 30 °C. The mixture was agitated at 180 rpm by a mechanical agitator (REMI), until the equilibrium condition was achieved. Aliquots of the dye solution were withdrawn at regular time intervals, centrifuged, and the supernatants were analyzed as mentioned above. Batch adsorption experiments were carried out by mixing 100 mg of PSPO with 100 mL of the dye solution of different initial concentration ranges for analyzing the effect of the initial dye concentration over the adsorption of the dyes on the PSPO. Also, the experimental data were used to test the different isotherm models to determine the adsorption mechanism. The amount of dye adsorbed, q_e (mg/g), was determined by using the following mass balance relationship:

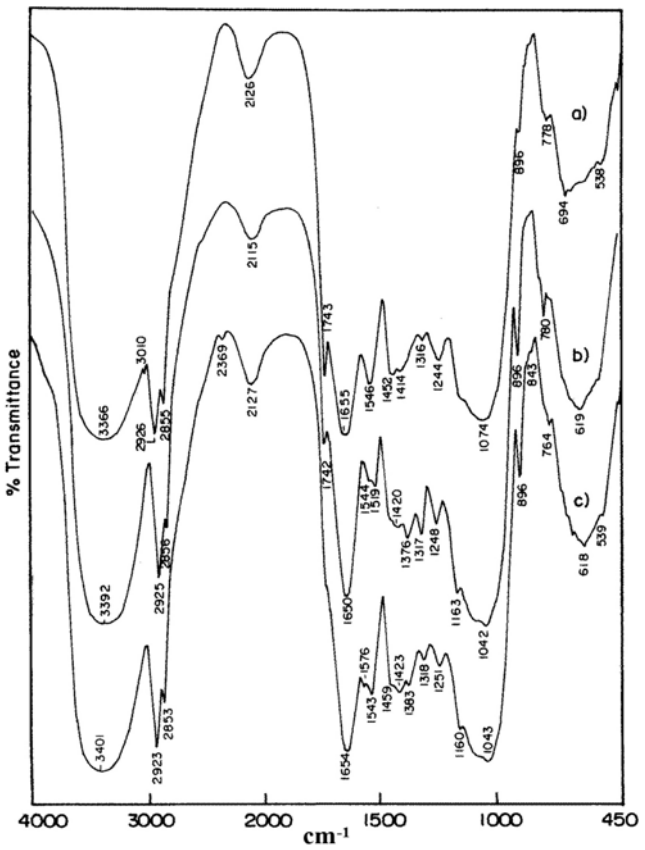

Fig. 2. (a) FT-IR spectrum of PSPO, (b) after MG adsorption and (c) after RB adsorption.

$$q_e = \frac{(C_i - C_e)V}{W} \quad (2)$$

where C_i and C_e are the initial and equilibrium concentrations (mg/L) of the dye solution respectively; V is the volume of dye solution (L); and W is the mass (g) of the adsorbent.

RESULTS AND DISCUSSION

1. Characteristics of PSPO

1-1. FTIR Studies

The FT-IR spectrum of the PSPO is shown in Fig. 2(a). The intense broad peak at 3,366 cm^{-1} is due to the O-H stretching vibration of the cellulose of plantago seeds. The presence of aromatic components in the PSPO is evidenced by a peak at 3,010 cm^{-1} due to the C-H stretching vibration. The alkyl groups in the PSPO give intense peaks due to the CH_2 stretching vibrations at 2,926 and 2,855 cm^{-1}. The presence of oil is verified by its C=O vibration at 1,743 cm^{-1}. Peaks due to the corresponding COO^- vibration occur at 1,244 cm^{-1}. The CH_2 bending vibrations give peaks at 1,414 cm^{-1} and about 1,370 cm^{-1}. The broad intense peak at 1,074 cm^{-1} is due to the C-O vibration of esters and alcoholic groups. The aromatic C-H bending vibration and CH_2 rocking vibration give an intense broad peak below 800 cm^{-1}.

The FT-IR spectrum of the MG adsorbed PSPO is shown in Fig. 2(b). The spectrum displays peaks similar to those of the PSPO. The adsorption of the MG on the PSPO is evident from the peak positions of the various vibrations. The O-H stretching vibration of the cellulose is shifted and the peak becomes narrow. Hence, the O-H group might aid the adsorption of MG by the hydrogen bonding interaction with the tertiary amino group. Again, the alkyl groups might also be involved in the adsorption of the MG, as there is a significant change in the intensity of the CH_2 stretching vibrations. The C-O vibration is also shifted by more than 30 cm^{-1} (from 1,074 to 1,042 cm^{-1}). The broad peak due to the aromatic C-H bending vibration is also narrow. The FT-IR spectrum of the RB adsorbed PSPO is shown in Fig. 2(c). It also displays features similar to those of the PSPO. Since the near disappearance of the C=O stretching vibration at 1,740 cm^{-1}, the ester groups of the oil in the seeds might be responsible for the adsorption of the RB. This is also evident from the shift of the COO^- vibration (1,244 cm^{-1}) of Fig. 2(a) to a higher value (1,951 cm^{-1}) as shown in Fig. 2(c). The peak maximum of the O-H stretching vibration is also shifted to a higher value. Both the dyes were adsorbed between cellulose matrices, which is verified from the narrowing of the aromatic C-H bending vibration.

1-2. Scanning Electron Microscopy (SEM)

The structural morphology of the adsorbent and the dye laden adsorbent were investigated by SEM analysis. The SEM images of the PSPO, the MG adsorbed PSPO and the RB adsorbed PSPO are shown in Figs. 3(a), 3(b) and 3(c), respectively. The irregular

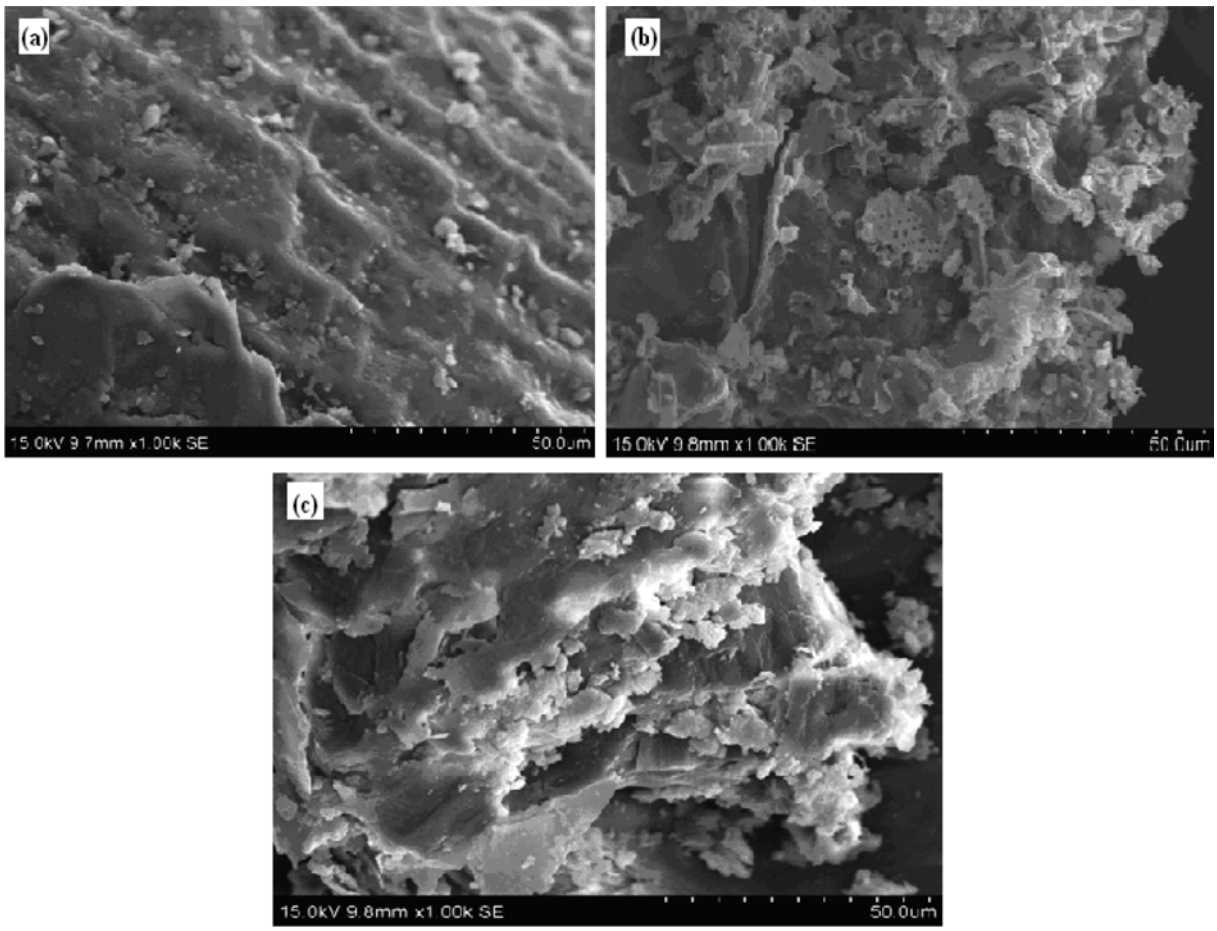

Fig. 3. SEM image of (a) PSPO; (b) SEM image of PSPO after MG dye adsorption; (c) SEM image of PSPO after RB dye adsorption.

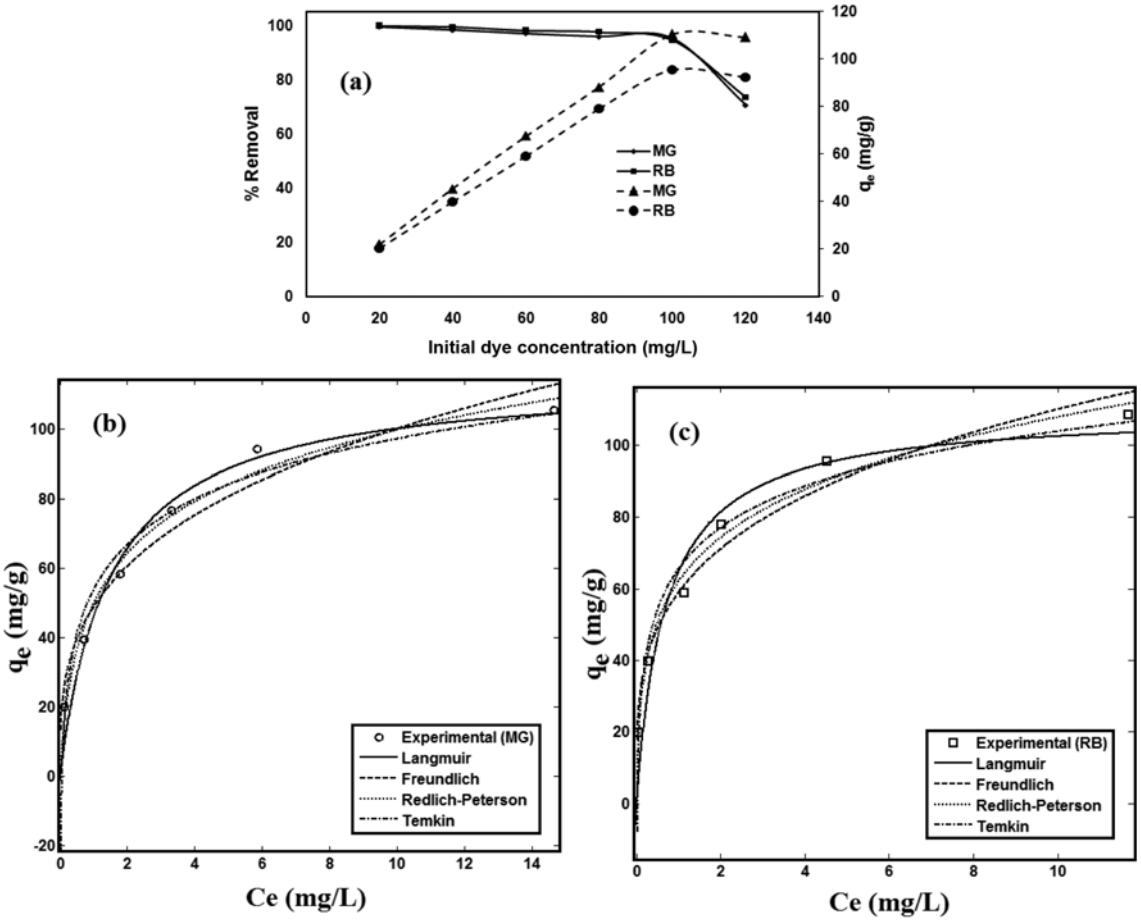

Fig. 4. Effect of (a) initial dye concentration (b) Non-linear adsorption isotherm for MG and (c) Non-linear adsorption isotherm for RB with PSPO at 30 °C.

surface of the adsorbent is inferred from Fig. 3(a). The irregular surface contributes to the large surface area of the adsorbent, which in turn influences the adsorbent capacity. The change in the morphology of the dye laden adsorbent observed in Figs. 3(b) and 3(c), when it is compared with the SEM image of PSPO (Fig. 3(a)), shows that the dye is adsorbed onto the adsorbent surface.

2. Effect of the Initial Dye Concentration

The effect of the initial dye concentration on the adsorption of the dyes on the PSPO was investigated in the range of 20 to 120 mg/L and the obtained result is shown in Fig. 4(a). It is evident that the percentage dye removal of the RB is be 99.774% for 20 mg/L of the initial dye concentration and 90.258% for 120 mg/L. Similarly, the percentage dye removal of the MG is 99.427% for 20 mg/L and 87.774% for 120 mg/L of the initial dye concentration. This variation in the results can be explained by the concentration gradient and also with adsorption capacity. The results show that the percentage of dye removal decreases with the increase in the initial concentration of the dye. The initial dye concentration provides the necessary driving force to overcome the resistance to the mass transfer of the dye between the aqueous phase and the solid phase. The increase in the initial dye concentration also enhances the interaction between the dye and the PSPO. Therefore, an increase in the initial dye concentration enhances the adsorption of the dye, due to the increase in the concentration gradient. However, the adsorbent capacity q_e shows an increase up to 100 mg/L and then decreases, because there would be a competition between the dyes in adsorbing, as the adsorbent pores get filled up by enough dye molecules, proving that a fixed dose of PSPO can only adsorb a certain amount of the dye.

3. Adsorption Equilibrium Study

The experimental data obtained from the effect of initial dye concentration studies were used to test the different adsorption isotherm models to know the adsorption mechanism. The adsorption isotherm plays an important role in the determination of the maximum adsorption capacity of the adsorbent. It also provides a panorama of the course taken by the system under study in a concise form, indicating how efficiently an adsorbent will adsorb and allow an estimate of the economic viability of the adsorbents for commercial applications. To adapt to the considered system, the isotherms of Langmuir, Freundlich, Redlich-Peterson and Temkin have been considered.

3-1. The Langmuir Isotherm

The theoretical Langmuir adsorption isotherm [10] is based on three assumptions: all the adsorbing sites over the surface of the adsorbent are equivalent and can accommodate at most one adsorbed atom; the ability of a molecule to adsorb at a given site is independent of the adsorption of the neighboring sites, and adsorption cannot proceed beyond a monolayer exposure. The non-linear equation

Table 1. Parameter values for each isotherm models used in the study

Isotherm model	RB			MG		
	Parameter	Values	R^2	Parameter	Values	R^2
Langmuir	q_m (mg/g)	109.4	0.9335	q_m (mg/g)	115.0	0.9668
	K_L (L/mg)	1.455		K_L (L/mg)	0.6696	
Freundlich	K_F((mg/g)(l/mg)$^{(1/n)}$)	59.03	0.9702	K_F((mg/g)(l/mg)$^{(1/n)}$)	48.97	0.9584
	n (g/L)	3.707		n	3.224	
Redlich-Peterson	K_R (L/g)	794.8	0.9846	K_R (L/g)	181.6	0.9784
	α_R (L/mg)	11.74		α_R (L/mg)	2.688	
	β	0.7909		β	0.8145	
Temkin	A	52.81	0.9724	A	17.76	0.9608
	B	7.183		B	8.14	

for the Langmuir isotherm model is expressed as follows:

$$q_e = \frac{q_m K_L C_e}{1 + K_L C_e} \quad (3)$$

where C_e is the dye concentration at the equilibrium state of the system (mg/L), q_m (mg/g) and K_L (L/mg) are the Langmuir constants, representing the maximum adsorption capacity for the solid phase loading, and the energy constant related to the heat of adsorption, respectively.

3-2. The Freundlich Isotherm

The Freundlich isotherm model [11] is a well known relationship describing the adsorption process. The assumptions of this model are that there is adsorption on heterogeneous surfaces with an interface between adsorbed molecules, and the adsorption energy exponentially decreases on satisfying the adsorption centers of the given adsorbent. This isotherm is an empirical equation which can be expressed as follows:

$$q_e = K_f C_e^{1/n} \quad (4)$$

where K_f is the Freundlich constant ((mg/g)(L/mg)$^{(1/n)}$) related to the bonding energy. K_f can be defined as the adsorption or distribution coefficient, and it represents the quantity of the dye adsorbed for unit equilibrium concentration. 1/n is the heterogeneity factor, and n is the gauge of the deviation from the linearity of adsorption. Its value indicates the degree of non-linearity between the solution concentration and adsorption as follows: if n=1, the adsorption is linear; if n<1, it implies that the adsorption process is favoured by chemisorption and if n>1, the adsorption process is favoured by physisorption.

3-3. The Redlich-Peterson Isotherm

The Redlich-Peterson isotherm is a combination of the Langmuir-Freundlich model. The equation is given as:

$$q_e = \frac{K_R C_e}{1 + \alpha_R C_e^{\beta}} \quad (5)$$

where K_R is the Redlich-Peterson isotherm constant (L/g), α_R is the Redlich-Peterson isotherm constant (L/mg), and β is the exponent which lies between 0 and 1. The constant β can characterize the isotherm; if β=1, the Langmuir will be the preferable isotherm, while if β=0, the Freundlich isotherm will be the preferable isotherm [12].

3-4. The Temkin Isotherm

The Temkin isotherm model [13] contains an aspect that overtly takes into account the adsorbent-adsorbate interactions. This model assumes the following: the heat of adsorption of all the molecules in the stratum decreases linearly with treatment due to adsorbent-adsorbate interactions, and the adsorption is characterized by a uniform allocation of binding energies, up to a maximum binding energy. The Temkin isotherm has been applied in the following form:

$$q_e = B \ln(AC_e) \quad (6)$$

where A and B are Temkin isotherm constants.

The experimental data on the effect of an initial dye concentration on the PSPO were fitted to the above adsorption isotherm models, and the graphical representations of these models are presented in Figs. 4(b) and 4(c) for the MG and RB, respectively. The constant values of the respective isotherms were calculated and given in Table 1 for both the dyes. From the Table 1, it is inferred from the Langmuir isotherm curve, that a saturated monolayer of dye molecules was adsorbed on the heterogeneous adsorbent surface, the energy of adsorption is constant and there is no migration of the adsorbate molecules on the surface plane. The value of n is found to be above unity from the Freundlich isotherm curve for both the dyes, and hence, adsorption is a favorable physical process. The Redlich-Peterson

Table 2. Comparison of adsorption capacity of various adsorbents for MG adsorption

Adsorbent	Adsorption capacity (mg/g)	References
PSPO	**115.00**	**Present study on MG**
PSPO	**109.40**	**Present study on RB**
Zea mays dust carbon	90.09	[14]
Rattan sawdust	61.00	[15]
Lemon peel activated carbon	42.18	[16]
Rubber wood sawdust	36.30	[17]
Banana peel	21.00	[18]
Rice husk	19.83	[19]
Borassus bark activated carbon	19.76	[20]
Date pits	17.30	[21]
Hen feather	10.70	[22]
Prawn waste	09.17	[23]
Commercial activated carbon	08.27	[24]

exponent β approaches nearer to 1 in the case of the MG and in the case of the RB. From the Redlich exponent data the adsorption of MG and RB follows the Langmuir isotherm preferably. The experimental data were also found to be in favor of the obtained data. The heat of the adsorption of the dye molecules in the stratum decreases linearly with coverage, due to adsorbent-adsorbate interactions, and the adsorption is characterized by a homogeneous allocation of binding energies, as preferably assumed from the Temkin isotherm. The comparison of the maximum monolayer adsorption capacity for the dyes MG and RB onto various adsorbents is presented in Table 2. It shows that the PSPO, studied in this work, has a large adsorption capacity when compared to other adsorbents, due to the more active sites present in the newly prepared adsorbent.

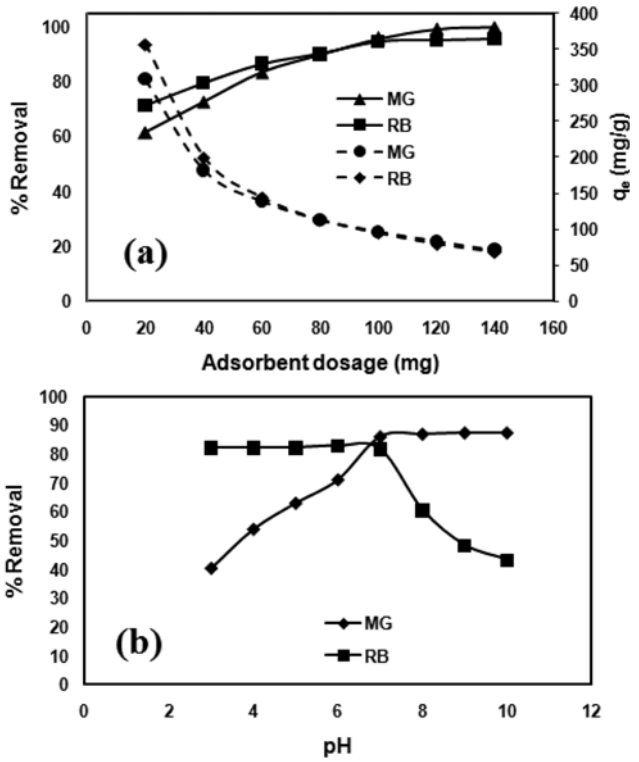

Fig. 5. Effect of (a) adsorbent dosage and (b) pH onto PSPO.

4. Effect of the Adsorbent Dose

To determine the optimum adsorbent dose, the effect of the adsorbent dosage on the dye removal was studied. Fig. 5(a) shows the results obtained from the experimental study and it is represented in terms of dye removal and the adsorption capacity q_e (mg/g) for different adsorbent doses. From the figure it is evident that the % of dye removal increases with an increase in the adsorbent dose, and there is a decrease in the adsorbent capacity. The % of dye removal increases from 54% to 99% and from 50% to 99% for the MG and RB, respectively, with respect to an increase in the adsorbent dose from 20 mg to 140 mg. At higher PSPO to dye concentration ratios, there is very fast superficial adsorption onto the PSPO surface, which produces a lower dye concentration in the solution, than when the biomass to dye concentration ratio is lower. As the adsorbent dose increases, there would be no dye molecules in the solution to be adsorbed; therefore, the adsorption sites remain vacant resulting in a decrease in the adsorption capacity.

5. Effect of the pH

The pH of the aqueous media influences the adsorptive uptake of dyes, because ionization or dissociation of the dyes could be altered by changing the pH of the aqueous media. The variation of the MG and RB adsorption on the PSPO over a pH range of 3 to 10 is shown in Fig. 5(b). At low pH values, the availability of H^+ and H_3O^+ ions is high in the solution, which leads the alkyl groups on the surface of the PSPO to acquire a positive charge by absorbing the H^+ and H_3O^+ ions. Since the PSPO surface is positively charged, a significantly strong electrostatic attraction appears between the positively charged PSPO surface and the anionic dye RB, which results in maximum adsorption. The % of dye removal of the RB decreases rapidly above the pH 7, as there will be a competition between the RB and the negative ions. As the pH of the system increases, the number of negatively charged sites increases and the number of positively charged sites decreases. A negatively charged surface site on the PSPO favors the adsorption of the cationic dye MG, due to the electrostatic attraction. But above pH 7, there is no profound increase in the % of dye removal. Hence, pH 7 is found to be the optimum for the maximum removal of both the dyes.

6. Effect of Contact Time

Studies on the effect of contact time on the removal of the dye by the PSPO show the rapid adsorption of the dye in the first 100

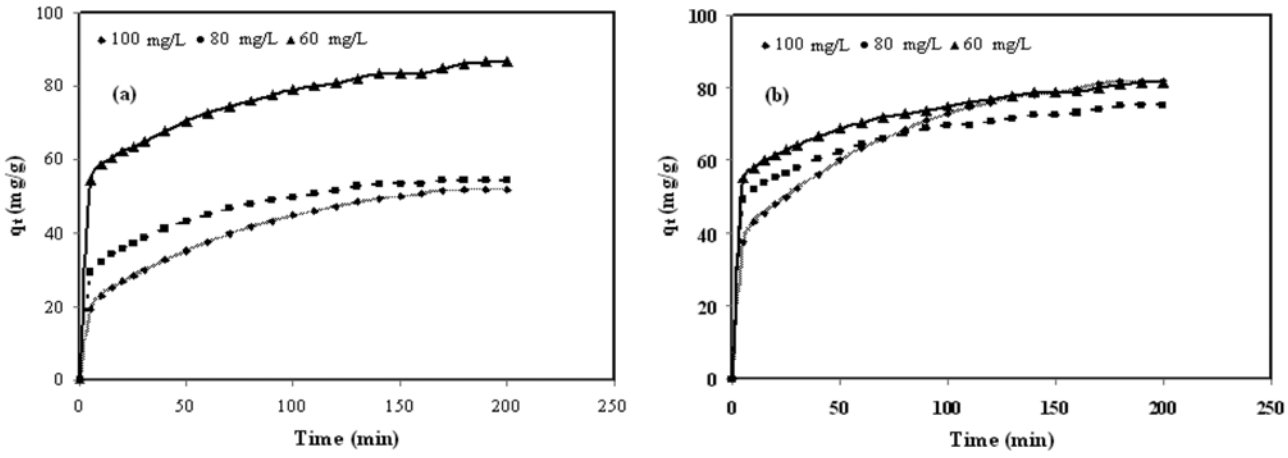

Fig. 6. Effect of contact time for the adsorption of (a) MG and (b) RB onto PSPO.

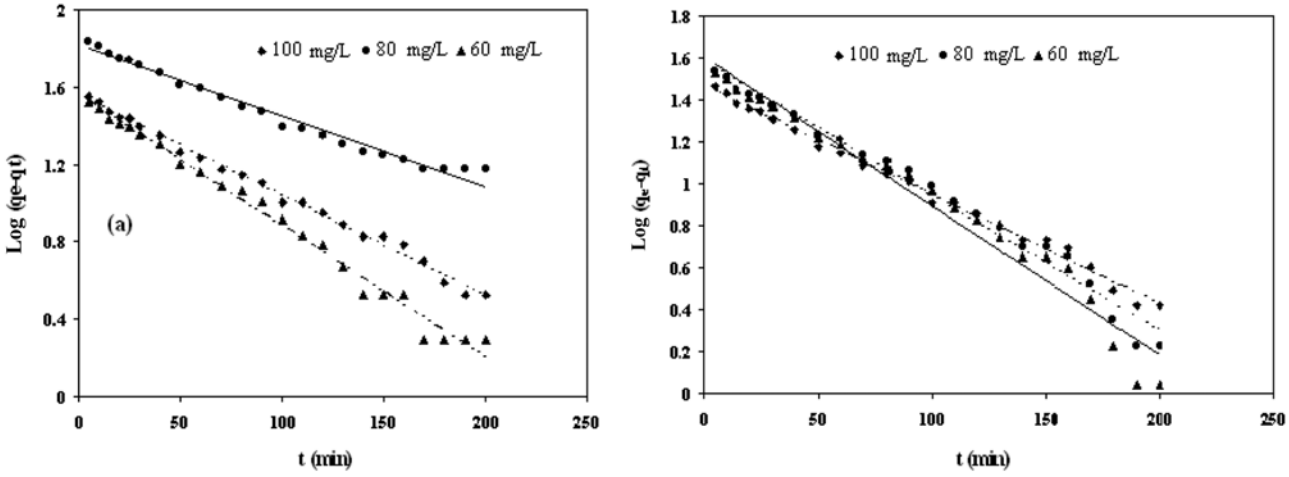

Fig. 7. Pseudo-first order kinetic fit for adsorption of (a) MG and (b) RB onto PSPO at 30 °C.

Table 3. Kinetic models and other statistical parameters at 30 °C and at pH 5

	Pseudo-first-order rate equation				Pseudo-second-order rate equation					Intraparticle diffusion		
Dyes	Conc (mg/L)	k_{ad} (min^{-1})	q_e (mg/g)	R^2	$q_{e,cal}$ (mg/g)	$q_{e,exp}$ (mg/g)	k (g mg^{-1} min^{-1})	h (mg g^{-1} min^{-1})	R^2	k_p (mg/g $min^{1/2}$)	C	R^2
MG	60	0.0069	40.18	0.981	90.90	86.66	0.00068	2.688	0.993	2.802	17.64	0.984
	80	0.0138	40.18	0.989	76.92	69.32	0.00082	4.854	0.996	2.802	32.07	0.986
	100	0.0012	35.89	0.993	62.50	54.89	0.00158	8.547	0.998	2.751	50.11	0.986
RB	60	0.0161	40.36	0.968	83.33	81.36	0.00089	3.07	0.990	2.802	51.44	0.982
	80	0.0138	38.55	0.994	76.92	67.32	0.00094	5.55	0.994	2.802	32.07	0.986
	100	0.0012	29.44	0.983	58.82	54.89	0.00016	10.99	0.998	2.256	17.64	0.986

min, and then, the adsorption rate stabilizes gradually and reaches equilibrium in about 200 min, as shown in Fig. 6. The aggregation of the dye molecules negates the influence of the contact time, as the adsorbent gets filled up and starts offering resistance to the diffusion of the dye molecules into the adsorbent. This is the reason why an insignificant enhancement in adsorption is effected in 200 min, as compared to that in 100 min. After 200 min contact, a steady state approximation was assumed, and a quasi-equilibrium situation was accepted. Further experiments were conducted for 200 min contact time only. The adsorption curves were single, smooth and continuous, leading to saturation, and indicate possible monolayer coverage on the surface of the adsorbent by the dye molecules.

7. Adsorption Kinetics

To examine the controlling mechanism of the adsorption process, the pseudo-first order and pseudo-second order kinetic equations were used to test the experimental data. The pseudo-first order kinetic model was suggested by Lagergren [25]. The pseudo-first order equation is given by,

$$\log(q_e - q_t) = \log q_e - \frac{k_{ad}}{2.303}t \quad (7)$$

where q_t is the adsorption capacity at time t (mg/g) and k_{ad} (min^{-1}) is the rate constant of the pseudo-first order kinetic equation.

The rate constant (k_{ad}), adsorption equilibrium capacity (q_e) and coefficient of determination (R^2) of both the dyes for different initial dye concentrations were calculated from the linear plots of log (q_e–q_t) versus t (Fig. 7(a)), and the values have been listed in Table 3.

The kinetic data were further analyzed using Ho's pseudo-second order kinetics model [26]. This model is based on the assumption that adsorption follows chemisorption. It can be expressed as:

$$\frac{t}{q_t} = \frac{1}{h} + \frac{1}{q_e}t \quad (8)$$

where (mg g^{-1} min^{-1}) is the initial adsorption rate at $t \rightarrow 0$ and k is the rate constant of the pseudo-second order kinetic equation (g mg^{-1} min^{-1}). The plot of t/q_t versus t is shown in Fig. 7(b). The q_e, k and h can be determined from the slope and intercept of the plot, respectively, and are listed in Table 3.

To gain an insight into the adsorption mechanism, the experimental data should be fitted to the mass transfer kinetic model, like Weber's intraparticle diffusion model [27]. This model is expressed as:

$$q_t = k_p t^{1/2} + C \quad (9)$$

where C is the intercept and k_p is the intraparticle diffusion rate constant (mg/g$min^{1/2}$), which can be evaluated from the slope of the linear plot of q_t versus $t^{(1/2)}$, (Fig. 7(c)). The intercept of the plot reflects the boundary layer effect. The larger the intercept, the greater will be the contribution of the surface adsorption in the rate controlling step. The calculated intraparticle diffusion coefficient k_p, C and R^2 values are listed in Table 3. Though the R^2 values are found to be high in both the pseudo-first order and pseudo-second order, the q_e experimental values are close to the q_e calculated values in the pseudo-

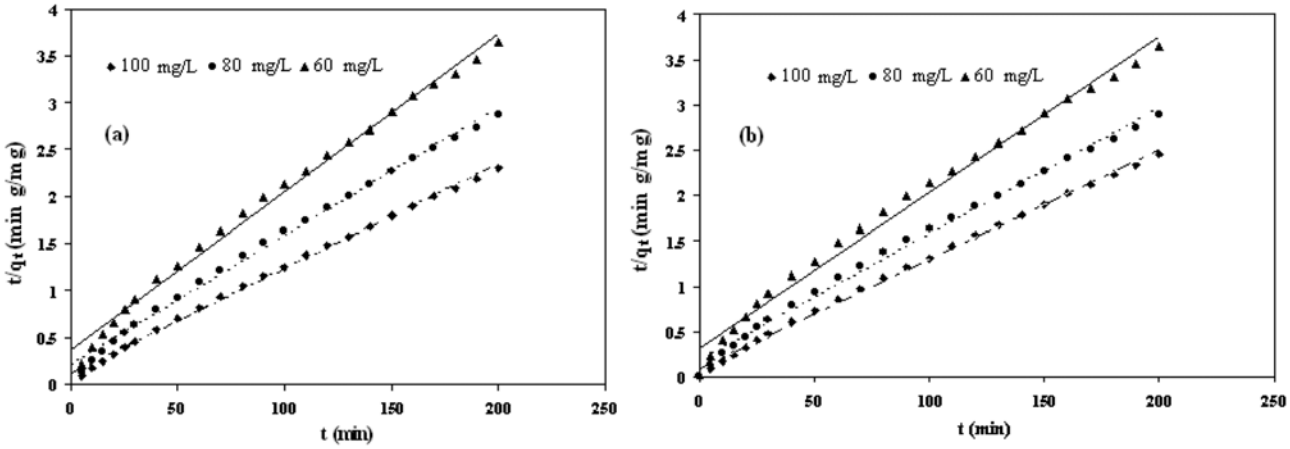

Fig. 8. Pseudo-second order kinetic fit for adsorption of (a) MG and (b) RB onto PSPO at 30 °C.

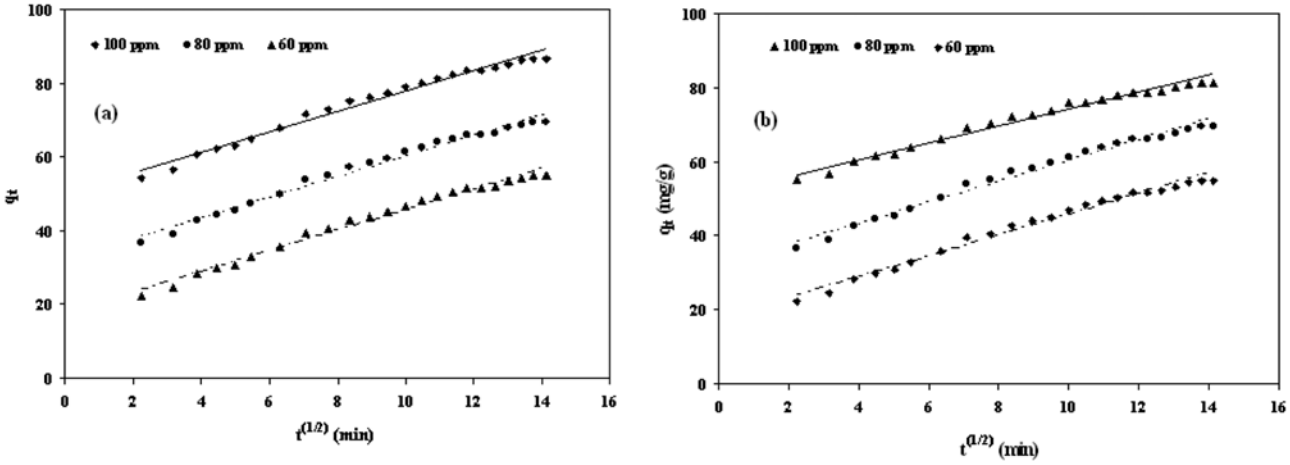

Fig. 9. Intraparticle diffusion model for adsorption of (a) MG and (b) RB onto PSPO at 30 °C.

second order model. Therefore, the rate-limiting step of the dyes on the PSPO may be due to chemisorption. In the diffusion model, if the plot of q_t versus $t^{(1/2)}$ (Fig. 7(c)) is linear and passes through the origin, then intraparticle diffusion is the sole rate-limiting step. However, the linear plots for both the MG and RB dyes did not pass through the origin. This indicates that intraparticle diffusion was not the only rate controlling step. Hence, it is concluded that the rate limiting step for the adsorption of the MG and RB dyes on the PSPO may be due to both chemisorption and intraparticle diffusion.

CONCLUSION

The seeds of *Plantago ovata* used in this investigation are available abundantly in India. The FTIR results show that the adsorbent could be a feasible option for its utilization in dye removal, due to the presence of cellulose matrices in the PSPO. The optimum value for the maximum removal of both the dyes was pH 7. The percentage of the dye removal of the RB decreases rapidly above pH 7, as there will be a competition between the RB and the negative ions, and above pH 7, there is no profound increase in the % of the dye removal for the MG. The percentage of dye removal increases from 54% to 99% and from 50% to 99% for the MG and RB, respectively, with respect to an increase in the adsorbent dose from 20 mg to 140 mg. At higher PSPO to dye concentration ratios, the adsorption sites remain vacant, resulting in a decrease of the adsorption capacity. The adsorbent capacity q_e shows an increase up to 100 mg/L and then decreases, because there would be a competition between the dyes in adsorbing, as the adsorbent pores get filled up by enough dye molecules. For the effect of contact time, equilibrium was achieved in 200 min. The suitability of the pseudo-first order, pseudo-second order and intra particle diffusion kinetic model for the adsorption of dyes on the PSPO has also been discussed. The pseudo-second order and intraparticle diffusion kinetic model agree well with the dynamic behavior of the adsorption of both the dyes on the PSPO. The equilibrium data have been analyzed using the Langmuir, Freundlich, Redlich-Peterson and Temkin isotherms. From the Redlich exponent data adsorption of MG and RB follows the Langmuir isotherm preferably. The experimental data was also found to be in favor of the obtained data. The adsorption capacity of the PSPO was found to be 115 mg/g and 109.4 mg/g for the MG and RB respectively. From this study, the PSPO was found to be a feasible adsorbent for the removal of dyes from aqueous solutions.

REFERENCES

1. T. F. Robinson, G. McMullan, R. Marchant and P. Nigam, *Biore-*

sour. Technol., **77**, 247 (2001).
2. J. Kent, Van Nostrand Reinhold, New York, N. Y. 7th Ed., 676 (1974).
3. P. J. Halliday and S. Beszedits, *Can. Tex. J.*, **103**, 78 (1986).
4. G. S. Gupta, G. Prasad and V. N. Singh, *Water Res.*, **24**, 45 (1990).
5. M. Neamtu, A. Yediler, I. Siminiceanu, M. Macoveanu and A. Kellrup, *Dyes Pigm*., **60**, 61 (2004).
6. I. K. Kapdan and R. Ozturk, *J. Hazard. Mater.*, **123**, 217 (2005).
7. R. K. Wahi, W. W. Yu, Y. P. Liu, M. L. Meija, J. C. Falkner, W. Nolte and V. L. Colvin, *J. Mol. Catal. A: Chem.*, **242**, 48 (2005).
8. V. V. B. Rao and S. R. M. Rao, *Chem. Eng. J.*, **116**, 77 (2006).
9. C. S. Keng, Z. Zainal and A. H. Abdullah, *J. Anal. Sci.*, **12**, 451 (2008).
10. I. Langmuir, *J. Ame. Chem. Soc.*, **40**, 1361 (1918).
11. H. M. F. Freundlich, *J. Phys. Chem.*, **57**, 385 (1906).
12. O. Redlich and D. L. Peterson, *J. Phys. Chem.*, **63**, 1024 (1959).
13. M. J. Temkin and V. Pyzhev, *Acta Physicochim. URSS*., **12**, 217 (1940).
14. P. K. Baskaran, B. R. Venkatraman and S. Arivoli, *E-J. Chem*., **8**, 9 (2011).
15. B. H. Hameed and M. I. El-Khaiary, *J. Hazard. Mater.*, **157**, 344 (2008).
16. K. V. Kumar, *Dyes Pigm.*, **74**, 595 (2007).
17. K. V. Kumar and S. Sivanesan, *Dyes Pigm.*, **72**, 124 (2007).
18. G. Annadurai, R. S. Juang and D. J. Lee, *J. Hazard. Mater.*, **B92**, 263 (2002).
19. N. Kannan and M. M. Sundaram, *Dyes Pigm.*, **51**, 25 (2001).
20. M. P. Hema and Martin Deva Prasath, *J. Sci. Eng.*, **34**, 31 (2009).
21. F. Banat, S. Al-Asheh and L. Al-Makhadmeh, *Process. Biochem*., **39**, 193 (2003).
22. Mittal and Alok, *J. Hazard. Mater.*, **133**, 196 (2006).
23. T. Santhi, S. Manonmani, T. Smitha and K. Mahalakshmi, *J. Chem.*, **2**, 813 (2009).
24. I. D. Mall, V. C. Srivastava, N. K. Agarwal and I. M. Mishra, *Colloids Surf*., **264**, 17 (2005).
25. S. Lagergren, *Kungliga Svenska Vetensk Handl.*, **24**, 1 (1898).
26. Y. S. Ho and G. McKay, *Process Biochem*., **34**, 451 (1999).
27. W. J. Weber and J. C. Morriss, *J. Sanit. Eng. Div. Am. Soc. Civ. Eng.*, **89**, 31 (1963).